Clim Dyn (2014) 42:271–290
DOI 10.1007/s00382-013-1671-6

Impacts of Indian Ocean SST biases on the Indian Monsoon: as simulated in a global coupled model

Chloé Prodhomme · Pascal Terray · Sébastien Masson · Takeshi Izumo · Tomoki Tozuka · Toshio Yamagata

Received: 14 August 2012 / Accepted: 15 January 2013 / Published online: 30 January 2013

Abstract In this study, the impact of the ocean–atmosphere coupling on the atmospheric mean state over the Indian Ocean and the Indian Summer Monsoon (ISM) is examined in the framework of the SINTEX-F2 coupled model through forced and coupled control simulations and several sensitivity coupled experiments. During boreal winter and spring, most of the Indian Ocean biases are common in forced and coupled simulations, suggesting that the errors originate from the atmospheric model, especially a dry islands bias in the Maritime Continent. During boreal summer, the air-sea coupling decreases the ISM rainfall over South India and the monsoon strength to realistic amplitude, but at the expense of important degradations of the rainfall and Sea Surface Temperature (SST) mean states in the Indian Ocean. Strong SST biases of opposite sign are observed over the western (WIO) and eastern (EIO) tropical Indian Ocean. Rainfall amounts over the ocean (land) are systematically higher (lower) in the northern hemisphere and the south equatorial Indian Ocean rainfall band is missing in the control coupled simulation. During boreal fall, positive dipole-like errors emerge in the mean state of the coupled model, with warm and wet (cold and dry) biases in the WIO (EIO), suggesting again a significant impact of the SST errors. The exact contributions and the distinct roles of these SST errors in the seasonal mean atmospheric state of the coupled model have been further assessed with two sensitivity coupled experiments, in which the SST biases are replaced by observed climatology either in the WIO (warm bias) or EIO (cold bias). The correction of the WIO warm bias leads to a global decrease of rainfall in the monsoon region, which confirms that the WIO is an important source of moisture for the ISM. On the other hand, the correction of the EIO cold bias leads to a global improvement of precipitation and circulation mean state during summer and fall. Nevertheless, all these improvements due to SST corrections seem drastically limited by the atmosphere intrinsic biases, including prominently the unimodal oceanic position of the ITCZ (Inter Tropical Convergence Zone) during summer and the enhanced westward wind stress along the equator during fall.

Keywords Indian Monsoon · Coupled climate model · Model systematic errors · Ocean atmosphere interaction · Arabian Sea

1 Introduction

The Asian Summer Monsoon is one of the most dominant tropical atmospheric circulations, and the economies and livelihood of the populations of India and Southeast Asia depend heavily on its rainfall (Wang 2006). Because of the dynamically interactive nature of the tropical Indo-Pacific ocean–atmosphere system, one of the best tools to study Indian Summer Monsoon (ISM) variability is a global Coupled General Circulation Model (CGCM). In order to provide reliable seasonal predictions and climate projections of monsoon rainfall, it is nevertheless essential that

C. Prodhomme · P. Terray · S. Masson · T. Izumo
LOCEAN-IPSL, CNRS, IRD, UPMC, MNHN, Paris, France

C. Prodhomme (✉)
LOCEAN-IPSL, Université Pierre et Marie Curie,
BP100, 4 Place Jussieu, 75252 Paris cedex 05, France
e-mail: chloe.prodhomme@locean-ipsl.upmc.fr

T. Tozuka · T. Yamagata
Department of Earth and Planetary Science,
Graduate School of Science, University of Tokyo, Tokyo, Japan

CGCMs are able to produce a reasonable simulation of the mean ISM circulation and rainfall distribution. Unfortunately, coupled climate modeling is still an area under rapid development, and CGCMs are still at a relatively early stage with most of the CGCMs exhibiting pervasive problems and deficiencies (Shukla et al. 2009). As an illustration, simulation of ISM and its variability still remains a significant challenge for many state-of-the-art CGCMs (Annamalai et al. 2007; Kripalani et al. 2007; Terray et al., 2005, 2012; Bollasina and Nigam 2009; Levine and Turner 2012). Out of the 22 CGCMs submitted to the World Climate Research Program's (WCRP) Coupled Model Intercomparison Project (CMIP) phase 3, Annamalai et al. (2007) and Kripalani et al. (2007) found, respectively, only six and seven models with a realistic ISM rainfall climatology. The large spread and difficulties of the CMIP3 CGCMs in simulating even the mean ISM rainfall during the 20th century add further doubts about the quality of the ISM rainfall projections by current CGCMs.

Even though current CGCMs simulate a substantially more realistic distribution of ISM rainfall compared to atmosphere-only models due to the importance of air–sea coupling in the monsoon variability (Wang et al. 2004, 2005, 2008; Kumar et al. 2005; Wu and Kirtman 2005), a major limiting factor for current CGCMs comes from model deficiencies in capturing the Sea Surface Temperature (SST) over the Indian Ocean, especially during boreal summer and fall. There is no doubt that SST variations over the Indian Ocean have significant impacts on ISM circulation and rainfall (Izumo et al. 2008; Annamalai 2010; Boschat et al. 2011, 2012), even though this role remains controversial (Annamalai and Murtugudde 2004). Therefore, important SST biases in coupled models drastically limit our understanding of the physical processes involved in the climate fluctuations, especially those associated with the ISM and Indian Ocean Dipole (IOD) (Bollasina and Nigam 2009; Fischer et al. 2005; Terray et al. 2012; Levine and Turner 2012).

Using the SINTEX-F2 coupled model, Joseph et al. (2012) hypothesized that the poor representation and weakness of ISM in this particular CGCM are due to a warm bias over the tropical Indian Ocean and the inherent weak meridional temperature gradient in the Indian region that drives the large scale monsoon flow (Chung and Ramanathan 2006). On the other hand, using the HadGEM3 CGCM, Levine and Turner (2012) suggest that cold SST biases over the Arabian Sea significantly reduce the ISM rainfall and circulation. This cold SST bias in the western Indian Ocean is pervasive in current CGCMs and may also drastically affect the simulated monsoon. The relationship between concurrent tropical Indian Ocean SSTs and ISM is thus controversial both in observations and current coupled simulations, partly due to the competing effects of SST on the evaporation and the meridional temperature gradient in the Indian region (Chung and Ramanathan 2006). These results warrant the need for improved monsoon and Indian Ocean SST simulations with current CGCMs.

These earlier studies provide the motivation for examining the roles of Indian Ocean SST biases on the ISM in a state-of-the-art CGCM, the SINTEX-F2 coupled model (Masson et al. 2012, Terray et al. 2012). As a first step toward the accurate coupled simulation of monsoon rainfall and Indian Ocean SST annual cycle, we have therefore examined the ability of this model to simulate the monsoon climate in both coupled and atmosphere-only configurations. Moreover, the present study includes the results of a group of sensitivity experiments with the CGCM, in order to unravel the specific roles of the Indian Ocean SST errors in the ISM rainfall and circulation simulation.

The paper is organized as follows. The model, the sensitivity experiments designed to study the specific role of SST biases in the western and eastern tropical Indian Ocean in the coupled simulation and the validation datasets used in this study are described in Sect. 2. In Sect. 3, we present the performance of the new version of the coupled model in simulating the monsoon climate in atmosphere-only and coupled configurations with a special emphasis on ISM and IOD. In Sect. 4, the results of the sensitivity experiments are analysed. The final section summarizes and discusses the main results of the present work.

2 Model and data description

2.1 SINTEX-F2 model

We have used the standard configuration of SINTEX-F2 model (Masson et al. 2012). It is the upgraded version of SINTEX-F1 CGCM (Guilyardi et al. 2003; Gualdi et al. 2003a; Luo et al. 2003, 2005). The oceanic component is NEMO (Madec 2008; Madec et al. 1998), using the ORCA05 horizontal resolution (0.5°), 31 vertical levels and including the LIM2 ice model (Timmermann et al. 2005). The atmospheric component is ECHAM 5.3 (Roeckner et al. 2003, 2004) with the T106 (1.125°) horizontal resolution and 31 hybrid sigma-pressure levels. A mass flux scheme (Tiedtke 1989) is applied for cumulus convection with modifications for penetrative convection according to Nordeng (1994). The coupling information, without any flux corrections, is exchanged every 2 h by means of the OASIS 3 coupler (Valcke 2006). See Masson et al. (2012) and Terray et al. (2012) for more details.

We run a 110 year control experiment (named CTL hereafter) with the coupled configuration of SINTEX-F2. At the same time, we have run an AGCM experiment

(named FOR hereafter) with the atmospheric-only configuration of SINTEX-F2, forced by Advanced Very High Resolution Radiometer (AVHRR) daily SST from 1982 to 2010, in order to assess the impact of the ocean–atmosphere coupling on the simulated Indo-Pacific climatology.

2.2 Design of the sensitivity experiments

In order to investigate more thoroughly the impacts of some key SST biases, described in Sect. 3, we performed two 50-year sensitivity coupled experiments with a strong SST nudging in the western Indian Ocean (FTW hereafter) and eastern Indian Ocean (FTE hereafter), respectively. More precisely, we used the standard configuration of the CGCM described previously without any flux corrections, except in the Western Indian Ocean (WIO) and Eastern Indian Ocean (EIO) boxes (see Fig. 1) where, following Luo et al. (2005), we applied a large negative feedback value ($-2{,}400$ W m^{-2} K^{-1}) to the surface heat flux. This value corresponds to the 1-day relaxation time for temperature in a 50-m mixed layer. A Gaussian smoothing is applied in a transition zone at the limits of the SST restoring domains (see regions between the plain and dotted boxes in Fig. 1).

For the FTW experiment, the SST damping is applied toward a daily climatology computed from the, AVHRR only, daily Optimum Interpolation SST (OISST) version 2 dataset for the 1982–2010 period (Reynolds et al. 2007). In the FTE experiment, we added a $+0.5$ °C offset value to this daily SST climatology. The choice to add a constant 0.5° offset factor comes from the uniform differences between the AVHRR OISST climatology and Tropical rainfall measuring mission Microwave Imager (TMI) version 4 3-day mean climatology (see http://www.ssmi.com/tmi/tmi_description.html, Wentz et al. 2000). This difference could be explained by the inability of AVHRR's satellite to see through clouds in this active convection area or to some coastal "pollution" in TMI data. Being doubtful about the exact reason of this difference, we choose to keep IOSST data for our experiments in order to have a longer time series for computing the SST climatology, but add to it a 0.5 °C constant factor in order to maximize the perturbation introduced in the FTE experiment.

This large correction using daily climatology completely suppresses the interannual and intraseasonnal SST variability in these regions. Our goal here is to understand at the first order how the biases in these regions impact the mean state. We assumed that the impact of the suppressed variability is negligible compared to the importance of the biases as far as the mean state is concerned. Furthermore, these corrections do not impact significantly the amplitude of the atmospheric variability in the region (not shown). All experiments and their acronyms are summarized in Table 1.

2.3 Reference datasets

For rainfall comparison between observations and the model outputs, we used the Tropical Rainfall Measuring Mission (TRMM) observations, specifically the 0.25° by 0.25° horizontal resolution merged 3B43 dataset, which is available from 1998 to 2010 (Kummerow et al. 2001; Huffman et al. 1997). For wind, wind stress and atmospheric temperature, we used the ERA-Interim reanalysis from 1989 to 2009, the latest global atmospheric reanalysis produced by the European Centre for Medium-Range Weather Forecasts (Dee et al. 2011). For SST, we used the AVHRR infrared satellite SST product from 1982 to 2010 (Reynolds et al. 2007). We also used TRMM Microwave Imager (TMI) from 1998 to 2008 (Wentz et al. 2000). This product has a much better spatiotemporal sampling of observations over the cloudy areas of the tropical Indian

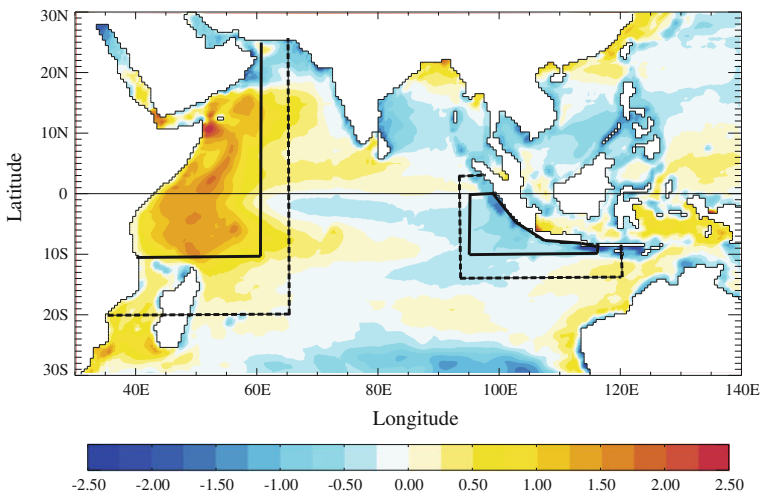

Fig. 1 Definition of the corrected areas in the sensitivity experiments on the top of SST difference between coupled experiment and observations from June to September. The *left* (*right*) *plain box* shows the delimitation of WIO (EIO) area. The *enclosing dotted box* shows the limit of the Gaussian smoothing applied in FTW (FTE)

Table 1 Summary of all experiments

Experiment's name	CTL	FOR	FTW	FTE
Type of experiment	CGCM	AGCM	CGCM	CGCM
Correction area	No correction applied	No correction applied	Western Indian Ocean (WIO): 35°E–60°E 10°S–30°N (see Fig. 1)	Eastern Indian Ocean (EIO): (see Fig. 1)
Observed data	No data	AVHRR	AVHRR	AVHRR + 0.5 °C
Time duration	110 years	29 years	50 years	50 years

Ocean, especially the eastern tropical Indian Ocean, than older products, because this sensor is nearly free of cloud interferences, but this product has a shorter time series than AVHRR. Finally, the Simple Ocean Data Assimilation (SODA) version 2.2.4 is used for diagnosing the 20° isotherm depth (used as a proxy for the thermocline depth) in the Indian Ocean (Carton and Giese 2008). SODA 2.2.4 covers the long period from 1871 to 2008 and uses winds from the new 20Crv2 atmospheric reanalysis (Compo et al. 2006), but we used only data from 1978 to 2008.

3 The monsoon annual cycle in observations, atmosphere-only and coupled runs

In this section, we compare the performances of the atmosphere-only (FOR) and coupled (CTL) configurations of SINTEX-F2 in simulating the annual cycle in the Indian areas. The focus here is to disentangle the biases, which are due specifically to the atmospheric model from those due to the ocean–atmosphere coupling in the coupled simulation of the monsoon cycle. More precisely, our aim is to identify the ≪atmospheric model errors≫, which are the errors in the atmospheric simulated fields, which can be detected in both the FOR and CTL simulations.

3.1 Boreal winter

During boreal winter (December to February), the observed latitudinal position of the InterTropical Convergence Zone (ITCZ) is around 5°S in the Indian Ocean and the rainfall distribution is organized in a southwest-northeast tilted band from Madagascar to the Maritime Continent (Fig. 2a). However, the main convection center is located over the Maritime Continent and the surrounding oceanic regions. Consistent with the rainfall distribution, the trade winds of both hemispheres converge around 5°S and the low level winds are westerly between the equator and 10°S in the Indian Ocean.

The coupled and forced experiments are successful in locating the mean ITCZ position during boreal winter (Fig. 2b, c). However, a striking feature is that both experiments share many errors. First, a dry bias is found over the islands of the Maritime Continent and, to a lesser extent, over Madagascar and North Australia in both experiments (Fig. 2e, f). Furthermore, both the coupled and forced runs show a wet bias over oceanic regions of the Maritime Continent, with unrealistically sharp land–sea contrasts. This suggests a significant underestimation of convective anomalies over the Maritime Continent, probably related to a misrepresentation of the strong diurnal cycle of convection over land in this area (related to small-scale phenomena like the land-sea breeze) and, also, to the very crude land model used in ECHAM (Alessandri et al. 2007; Neale and Slingo 2003). This large decrease of rainfall over the land of the Maritime Continent is associated with a pair of low-level anticyclonic anomalies straddling the equator in the central Indian Ocean and a consistently too weak westerly flow on and south of the equator during December-February (Fig. 2e, f). All these features can be attributed to Rossby wave responses to decreased diabatic heating over the Maritime Continent associated with the dry bias (Gill 1980). Another striking similarity between the two runs is a decreased low-level northeasterly flow over the Arabian Sea, suggesting a too weak winter monsoon. This is again consistent with a Gill atmospheric response to the decrease of precipitation over the Maritime Continent.

Focusing now on the differences between CTL and FOR, we note that the Indian Ocean ITCZ is too zonal and more active in CTL, especially over the western Indian Ocean and between Australia and Java (Fig. 2d, e). On the other hand, in FOR, a reduction of rainfall is seen over the eastern Indian Ocean with an opposite excess of precipitation from the African coast to the central south Indian Ocean (Fig. 2d).

These distinct rainfall patterns, over the South West Indian Ocean, in FOR and CTL simulations, are consistent with the simulated wind pattern (Fig. 2e, f). As an illustration, the erroneous low-level wind pattern simulated in the southern tropical Indian Ocean (induced by the heating errors over the Maritime Continent) implies that the

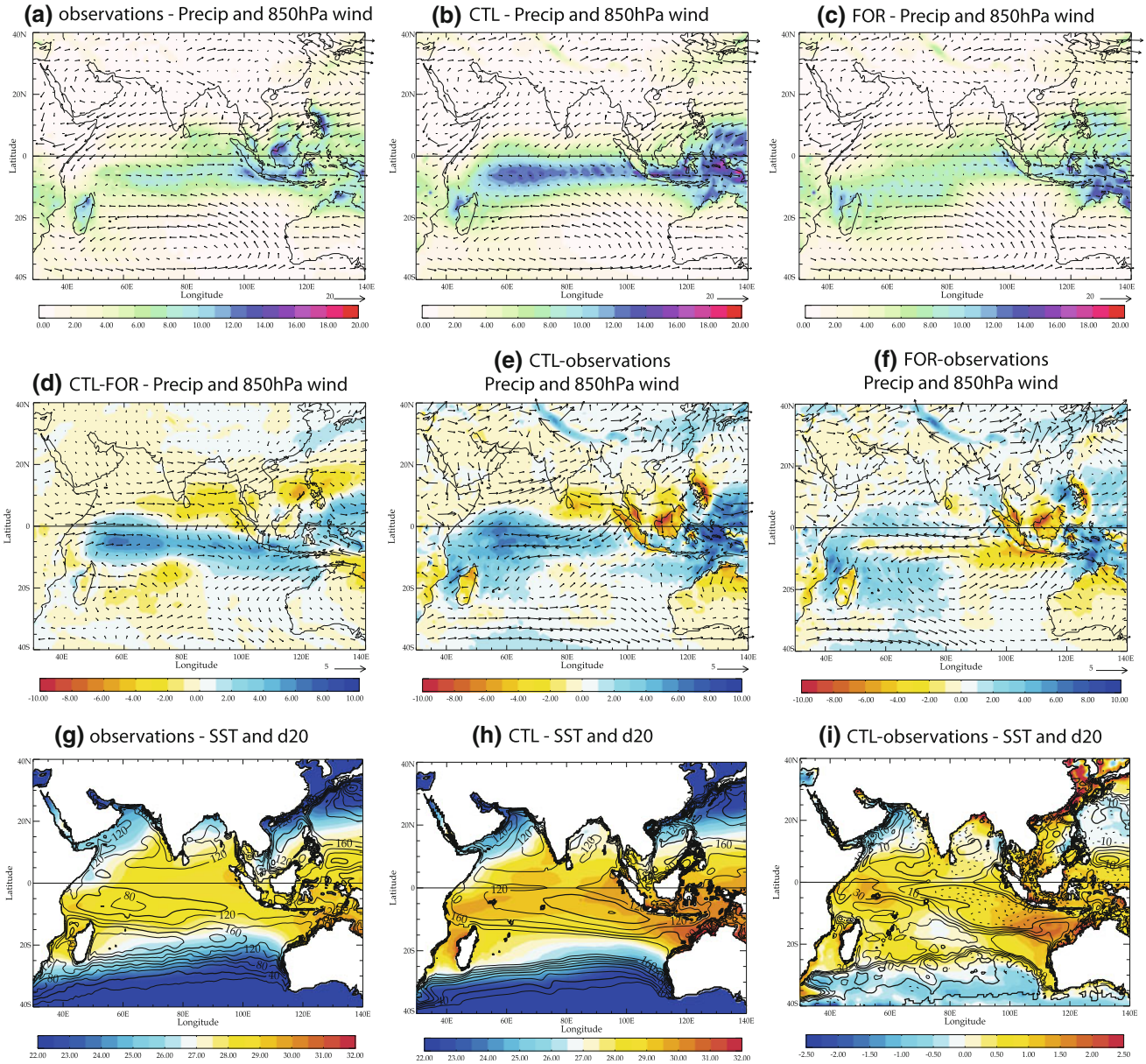

Fig. 2 **a** Observed climatology of precipitation (*shaded*, unit in mm/day, contour interval: 1 mm/day) and 850 hPa winds (*arrows*, unit in m/s) from December to February. The precipitation and low-level winds climatologies are estimated from the 1998–2010 and 1989–2009 periods, respectively. **b** Same as **a**, but for CTL. **c** Same as **a**, but for FOR. **d** Difference between CTL and FOR boreal winter climatologies for precipitation and 850 hPa winds. **e** Same as **d**, but for CTL minus observations climatologies. **f** Same as **d**, but for FOR minus observations climatologies. **g** Climatology of SST (*shaded*, unit in °C, contour interval: 0.5 °C) and depth of 20 °C isotherm during boreal winter (contour in m, contour interval: 20 m, contour min: 0 m, contour max: 200 m) for observations. The SST and depth of 20° isotherm climatologies are estimated from the 1998–2008 and 1978–2008 periods, respectively. **h** Same as **g**, but for the CTL. **i** Difference between CTL and observations boreal winter climatologies of SST (*shaded*, unit in °C, contour interval: 0.25 °C) and 20 °C isotherm depth (unit in m, contour interval: 10 m, contour min: −50 m, contour max: 50 m)

minimum of the wind stress curl is significantly shifted eastward in the simulations compared to the observations (not shown). Consistent with the work of Yokoi et al. (2008), this leads to an eastward shift in the location of the thermocline dome in the South tropical Indian Ocean in the coupled run (Fig. 2h, i). Finally, this feature may, in turn, explain the warm SST bias over the southwest tropical Indian Ocean and provides an explanation for the excessive precipitation in the western Indian Ocean during this season in CTL (Fig. 2d, i).

Over the far south-eastern Indian Ocean, Fig. 2i, f show an excess of precipitation and a warmer than observed SST. This suggests a driving role of the ocean in this region. Koch-Larrouy et al. (2007) show that the misrepresentation

of the tidal mixing in the OPA8.2 model is partly responsible of the warm SST bias in this region. The same mechanism could explain the warm bias in the south-eastern Indian Ocean, which, by an error compensation, attenuates the dry bias observed in this region in FOR.

To conclude about this season, the common errors in CTL and FOR suggest that most of the rainfall and circulation biases in the coupled run are driven by errors in the atmospheric model, especially over the Maritime Continent. The warmer SST in the south-eastern Indian Ocean in CTL (Fig. 2i) corrects the dry bias observed in FOR over this region thanks to an error compensation. However, the coupling also increases some biases: the erroneous low-level wind pattern in the south tropical Indian Ocean causes a warmer SST in the south-western Indian Ocean consistent with a stronger excess of precipitation over this region (Fig. 2i).

3.2 Boreal spring

Moving to the boreal spring (March to May), the latitudinal position of the ITCZ over the Indian Ocean is slightly shifted northward compared to boreal winter, in observations (Fig. 3a) and FOR (Fig. 3c), but less so in CTL (Fig. 3b) in which the rainfall band is still locked between 5 and 10°S (Fig. 3b, e). Both experiments successfully

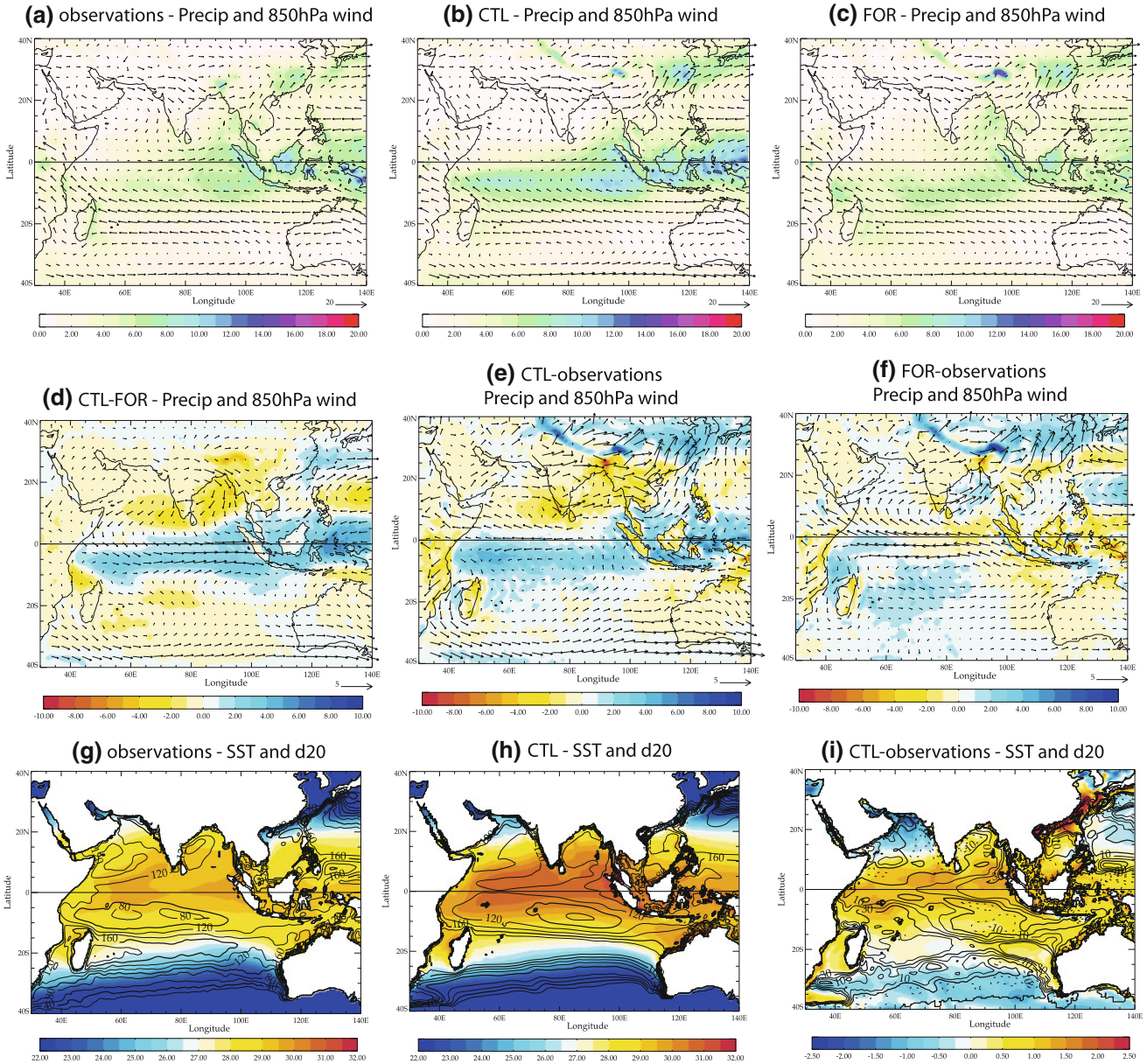

Fig. 3 Same as Fig. 2, but for boreal spring (March to May)

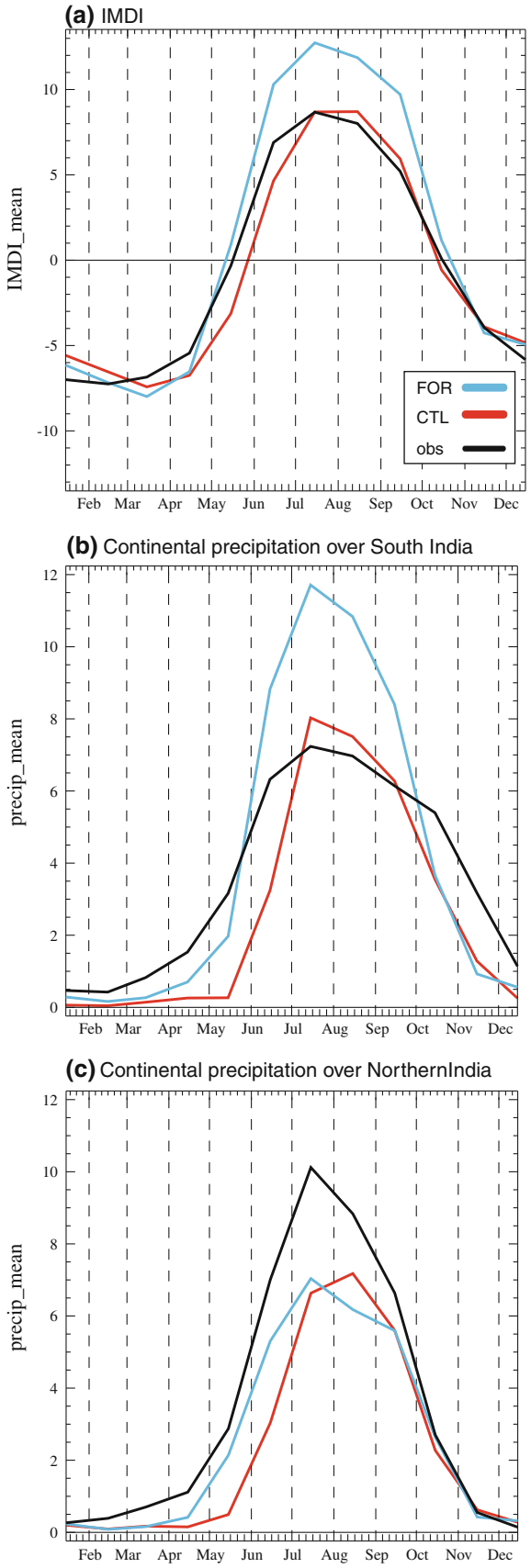

◀**Fig. 4** Annual cycle of different ISM rainfall and dynamical indices in observations, atmosphere-only and coupled experiments. **a** Monthly climatology of the Indian summer Monsoon Dynamical Index (IMDI) of Wang et al. (2001), defined as the difference of 850 hPa winds averaged between 5–5°N/40–80°E and 20–30°N/70–90°E. **b** Monthly climatology of precipitation (in mm/day) over South India between 70°E–90°E 5°N–20°N (e.g. excluding the ocean grid-points). **c** Monthly climatology of precipitation (in mm/day) over North India between 70°E–90°E 20°N–25°N (e.g. excluding the ocean grid-points). For all figures, observations are shown in *black* (precipitations are derived from TRMM from 1998 to 2010 and winds are derived from ERA interim from 1989 to 2009). CTL and FOR are shown in *red* and *light blue*, respectively

reproduced the monsoon's onset over East Asia, but with a too strong monsoon flow over the Bay of Bengal and East Asia (Fig. 3e, f). However, the dry bias located over the Maritime Continent during the previous winter season is still present with an unrealistic sharp rainfall land-sea contrast in this region in CTL. Moreover, the Gill atmospheric response to this dry bias, with low-level anticyclones over the central Indian Ocean in each hemisphere, is also detectable, especially in FOR (Fig. 3e, f). As a consequence, most of the thermocline and SST biases observed over the tropical Indian Ocean during boreal winter are also found during spring in CTL (Fig. 3i).

A distinctive feature of the CTL simulation during boreal spring is the persistence of the boreal winter anticyclonic pattern over the Arabian Sea and the associated dry bias over Kerala and the surrounding ocean (Fig. 3e). These rainfall and wind patterns suggest a delayed monsoon onset over Kerala and Myanmar in CTL. Figure 4 shows the observed and simulated mean annual cycle of various ISM rainfall indices and of the Indian Monsoon Dynamical Index (IMDI, difference in 850 hPa zonal winds averaged over 5–15°N/40–80°E and 20–30°N/70–90°E, Wang et al. 2001). The ISM onset normally occurs at the end of May over peninsular India in nature: this is well illustrated by the change of sign of IMDI (e.g. the reversal of the zonal wind shear in the Indian region) and the increase of precipitation over South India in May–June in observations (Fig. 4). The onset phase of ISM seems to be more realistic in FOR than in CTL, both from the point of view of the rainfall and dynamical indices, even though the amplitude of the summer monsoon is too strong in FOR. On the other hand, the ISM onset is delayed in CTL.

One hypothesis is that the delayed ISM onset in the coupled run is mostly attributable to the SST, thermocline, rainfall and low-level wind errors simulated in the western Indian Ocean during the pre-onset phase, which, in turn, are associated with the atmospheric circulation errors described for the preceding season (Joseph et al. 2003; Annamalai et al. 2005; Sijikumar and Rajeev 2012). This

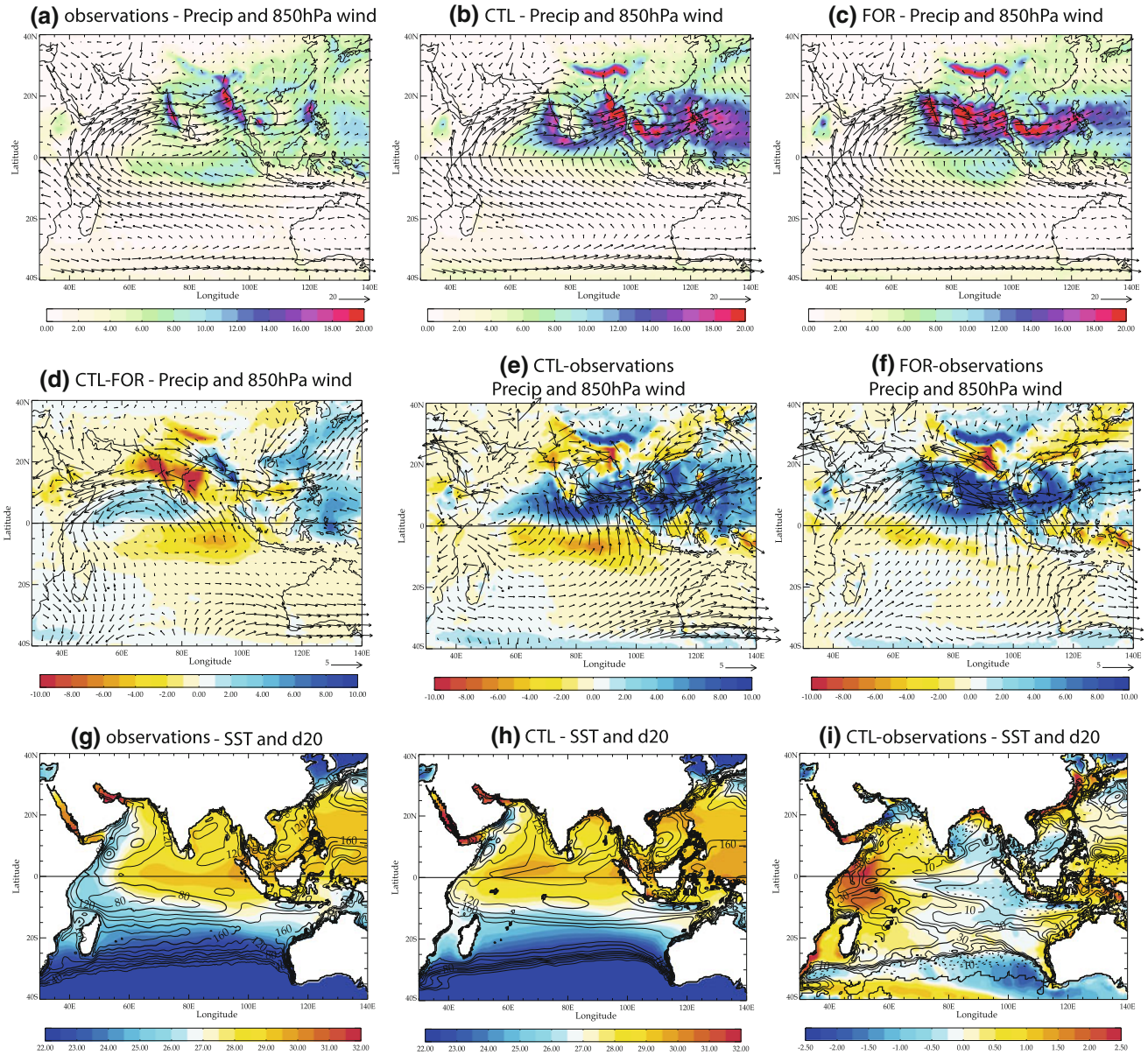

Fig. 5 Same as Fig. 2, but for boreal summer (June to August)

hypothesis will be tested more thoroughly with the help of dedicated sensitivity experiments in the next section.

To conclude about this transition season, many of the simulated rainfall and low-level wind errors may be again attributable to errors in the atmospheric model, especially the misrepresentation of convection over Maritime Continent islands and the associated Gill response to the lack of precipitation over this region.

3.3 Boreal summer

During the boreal summer (June–August), the pair-wise differences between observations, CTL and FOR are significantly enhanced (Fig. 4d, f) suggesting that, during ISM, the biases found in CTL are not solely due to errors in the atmospheric model. The dry islands bias in the Maritime Continent is still found during boreal summer, but is no longer the main rainfall errors in both simulations. This reinforces the hypothesis of a driving role of SST errors or the amplification of atmospheric errors by positive ocean–atmosphere feedbacks during this season.

Consistent with the results of Joseph et al. (2012) and Terray et al. (2012), CTL fails to simulate the rainfall band over the southeast equatorial Indian Ocean, which plays a prominent role in the intraseasonal ISM variability (Annamalai 2010; Krishnan et al. 2000). Interestingly, this important bias is less detectable in FOR and is collocated with a cold SST bias in CTL suggesting an impact of the

ocean–atmosphere coupling (Fig. 5d). However, CTL and FOR also share many deficiencies, including excessive precipitation over the Indian Ocean just north of the equator, a southward bias in the mean position of the ITCZ in the northern hemisphere and a dry bias above 20°N, especially over North India (Fig. 5e, f). All these common errors are also clearly illustrated in the annual cycle of different regional monsoon rainfall indices (Fig. 4). Thus, the incorrect position of the ITCZ can therefore not be related only to the major SST biases in CTL (in contradiction with the hypothesis of Joseph et al. 2012). These rainfall errors are a long-standing problem in the ECHAM atmospheric model (Roeckner et al. 1996, Cherchi and Navarra 2007).

Concerning the low level winds, both FOR and CTL are able to simulate a reasonable monsoon circulation, including a realistic monsoon trough (Fig. 5b, c). However, Fig. 5e, f demonstrate that the Somali jet is not confined near the African coast and the southern trade winds cross the equator from 40° to 100°E in both simulations. This bias is consistent with excessive/less precipitation just north/south of the equator in both simulations (Fig. 5e, f). This common error is however more pronounced in CTL than FOR (Fig. 5d), in addition, the ISM circulation is weaker in CTL (see also Fig. 4a), which is consistent with the lack of precipitation over central and north India in CTL compared to FOR (Figs. 4, 5d). The weaker monsoon strength in CTL, in response to weakened diabatic heating in the monsoon trough, is a clear improvement of mean wind circulation (see Fig. 4a) and highlights the impacts of the ocean–atmosphere coupling on the simulation of ISM (Wang et al. 2005; Kumar et al. 2005; Cherchi and Navarra 2007).

Since the coupling induces important changes in the simulated atmospheric and rainfall mean state, it is interesting to investigate the possible links between Indian Ocean SST biases and ISM circulation in the coupled simulation (Fig. 5g, i). The clear dipole structure of SST biases with a warm bias in the Western Indian Ocean (WIO, see Fig. 1) and a cold bias in the Eastern Indian Ocean (EIO, see Fig. 1) drives us to analyse these two regions separately.

In the WIO, the part of the warm SST bias located south of the Equator is consistent with the SST errors noted during the previous seasons and can be explained by the same mechanisms. North of the Equator, the poor representation of the Somalia upwelling (Schott et al. 1997; Schott and McCreary 2001) is very likely the cause of the warm SST bias, as documented in previous versions of SINTEX (Gualdi et al. 2003b). The reasons of the poor representation of the upwelling are not clear, the low resolution of the oceanic component could explain a part of the error, but the inability of the CTL run to reproduce a correct wind stress profile along the coast, especially the tangent component of the wind stress, is also a possible reason. Furthermore, the delayed ISM onset in CTL could also contribute to the reinforcement of this warm bias in the whole WIO during the first part of ISM. The SST bias in WIO appears to dominate the SST east–west gradient error in the equatorial Indian Ocean. In this respect, several recent studies have suggested a possible impact of SST in the western Arabian Sea on precipitation over India (Izumo et al. 2008; Levine and Turner 2012; Joseph et al. 2012). Izumo et al. (2008) and Levine and Turner (2012) show that cold (warm) SST biases in the WIO could decrease (enhance) monsoon rainfall in their coupled model. On the other hand, Joseph et al. (2012) suggest that the warm SST biases in the WIO could explain the weakness of the monsoon, north of 20°N, in SINTEX-F2, by setting up an erroneous meridional tropospheric temperature gradient in the Indian region (Chung and Ramanathan 2006). In other words, it is rather difficult to relate excessive precipitation over the Indian Ocean (just north of the equator) and the lack of precipitation over north India during ISM with the WIO SST errors in CTL. This question will be investigated in Sect. 4, with the help of the FTW experiment.

Focusing now on the EIO, the cold SST bias is clearly consistent with the lack of precipitation over this region in CTL and has also been a long-standing problem in the SINTEX coupled model (see Fig. 5i; also Fischer et al. 2005; Terray et al. 2012). But, again, it is not obvious to relate this SST bias with the precipitation and wind patterns observed to the north of the equator in the coupled model. Annamalai (2010) shows with a forced linear baroclinic model that the equatorial EIO SST could have an important impact on precipitations over north of India and Bay of Bengal. We will also go back to this problem with the FTE experiment in Sect. 4.

In summary, FOR and CTL share many biases mainly linked to an incorrect position of the ITCZ during boreal summer. On the other hand, the coupling induces important changes with a significant reduction of the ISM strength, but also a severe deficit of precipitation off Sumatra and Java and excessive rainfall over the WIO. The possible impact of the SST errors on the ISM rainfall and circulation in the Northern Hemisphere is not clear in CTL and will be addressed in the following section.

3.4 Boreal fall

During fall, the ITCZ moves from its northern position (around 20°N) to its southern position (around 5°S) in the Indian areas. The amplitude of the biases decreases significantly in FOR whereas the biases have the same intensity compared to the previous boreal summer in CTL (Figs. 5, 6). In contrast to the boreal summer, the coupling

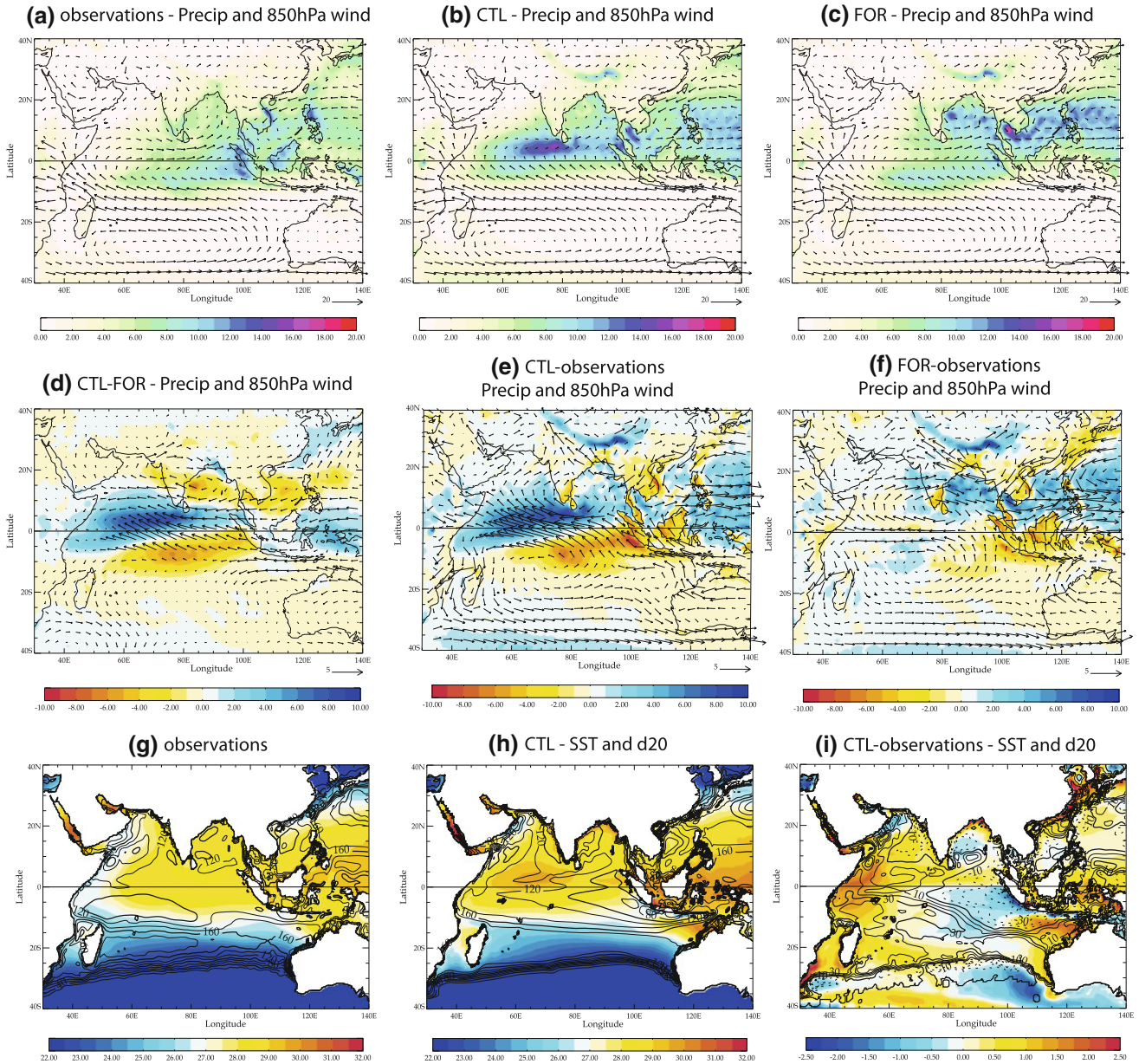

Fig. 6 Same as Fig. 2, but for boreal fall (September to November)

seems to have a negative impact on the simulated circulation and precipitation patterns during boreal fall.

In FOR, the southward shift of the ITCZ is significantly delayed as illustrated by the positive (negative) rainfall biases in the Bay of Bengal and China Sea (in the south-eastern Indian Ocean and Maritime Continent) in Fig. 6f. This is consistent with the persistence of the ISM circulation in the northern hemisphere (Fig. 6f) and the positive values of the IMDI in September–October (Fig. 4a) in this simulation. Consistent with delayed southward migration of the ITCZ and the dry islands bias in the Maritime Continent, FOR is affected by a very strong easterly wind bias over the equatorial Indian Ocean during boreal fall.

In CTL, the mean state of the Indian Ocean during fall is significantly degraded since amplitude of the SST and 20 °C isotherm biases have significantly increased from summer to fall (Fig. 6d, e). This is consistent with the existence of positive ocean–atmosphere feedbacks (Li et al. 2003; Chang et al. 2006; Terray et al. 2007). These positive IOD-like SST and thermocline patterns, already described by Terray et al. (2012) and also in an older version of SINTEX by Fischer et al. (2005), are accompanied by collocated rainfall biases with positive (negative) rainfall anomalies in the WIO (EIO) (Fig. 6e). Thus, as during positive IOD events in observations, the reversed SST equatorial gradient (Fig. 6h) induces a large-scale moisture

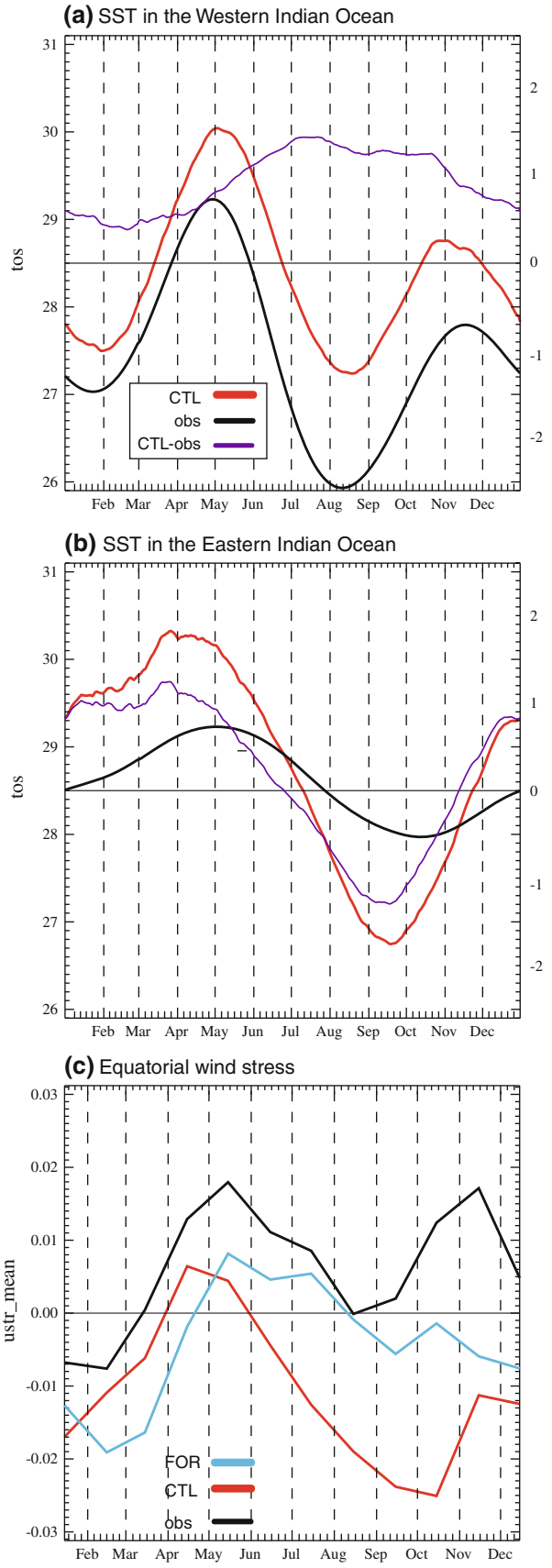

◀ **Fig. 7** Annual cycle of WIO and EIO SSTs and Indian Ocean equatorial wind stress in observations, atmosphere-only and coupled experiments. **a** Monthly climatology of SST (in °C) averaged in the WIO (35°E 60°E–10°S 30°N). **b** Monthly climatology of SST (in degree Celsius) averaged in the EIO (see the *specific box* shown on Fig. 8). For **a** and **b**, observations are derived from AVHRR from 1998 to 2010 and are shown in *black*. CTL is shown in red and the difference between CTL and observation is shown in *purple* with the scale indicated on the *right* side of the plot. **c** Monthly climatology of zonal wind stress (N/m^2) averaged between 40°E–10O°E and 5°S–5°N. Observations are derived from ERA interim from 1989 to 2009 and shown in *black*. CTL and FOR are shown in *red* and *light blue*, respectively

convergence, leading to the local build-up of deep convection over the south Arabian Sea and the existence of low-level weak easterly winds over the equator during fall in CTL, instead of the observed westerly winds (Fig. 6a, b; see also Fig. 7c). The strength and persistence of this IOD-like wind-SST-thermocline feedback in CTL may explain why the ITCZ stays locked in the south Arabian Sea, instead of moving southeastward as in the forced simulation and the observations (Fig. 6d, e).

The importance of IOD-like air-sea interactions during this season hints an important and retroactive forcing of SST onto the atmospheric circulation in CTL. Figure 7 shows that the enhancement of the warm bias in the WIO, in the early summer, occurs simultaneously with the degradation of the equatorial wind stress in CTL and is closely followed by the formation of the cold bias in the EIO. This suggests that the WIO SST bias may be responsible of the emergence of the EIO SST bias during boreal summer and fall, for example via equatorial wind stress forcing, as in some positive dipole events (during El Niño years) in which the warming of the WIO is the major feature and governs the evolution of the event (Loschnigg et al. 2003; Drbohlav et al. 2007; Boschat et al. 2012). We will also address this question in more details in the next section.

To conclude this section, the comparison of seasonal cycles in FOR, CTL and observations suggests that, during boreal winter and spring the main source of errors is the atmospheric model, including prominently land surface and coastal processes (e.g. land-sea breeze) over the islands of the Maritime Continent. During summer and fall, the SST biases seem to have a more significant impact on the oceanic and atmospheric circulation errors. We will, in the next section, investigate more thoroughly these impacts with two dedicated sensitivity coupled experiments.

4 Sensitivity experiments

In this section, we will investigate more thoroughly how WIO and EIO SSTs impact the mean state during summer

and fall with two sensitivity coupled experiments: FTE and FTW (described in Sect. 2.2, and summarized in Table 1). With the help of these two sensitivity experiments, we will try to answer specifically the following opened questions, which emerge from the previous analyses:

1. What is the exact contribution of WIO and EIO SST biases to the various deficient features affecting the ISM rainfall and circulation, including the delayed ISM onset and the wrong position of the ITCZ, during boreal summer in the CGCM?
2. What are the exact contributions of WIO and EIO SST biases in the emergence of the positive dipole-like structure in the mean-state of the CGCM during boreal fall?

To simplify the presentation of the results, we will first discuss the results related to the ISM rainfall and circulation and then address the problem of the emergence of the dipole-like structure in the boreal fall mean-state of the CGCM.

4.1 Impact of SST biases on ISM onset, rainfall and circulation

4.1.1 ISM onset

The monsoon onset is often represented by various indices defined from rainfall as well as dynamical parameters. Following the work of Xavier et al. (2007), we use a thermodynamical index based on the tropospheric temperature gradient (hereafter referred as Tropospheric Temperature Gradient (TTG) Index) to find out the onset of monsoon season. More precisely, the TTG index is defined by the difference in the tropospheric temperature (TT; defined as the temperature averaged between 600 and 200 hPa) between a northern box (40°–100°E; 5°–35°N) and a southern box (40°–100°E; 15°S–5°N). The onset of the monsoon is then defined when the value of TTG becomes positive from negative. The monsoon onsets in Julian days are 148, 142 and 158 in observations (ERA interim), FOR and CTL simulations, respectively. In other words, the monsoon onset is significantly delayed in CTL compared to observations and FOR, as suggested in Sect. 3.

Surprisingly, the ISM rainfall onset over the land remains delayed in both the FTW and FTE experiments as in CTL (Fig. 8a). Furthermore, the monsoon onset (in Julian days), as determined from the TTG index, is 155.6 and 158 in FTW and FTE, respectively. While these results may be expected for the FTE experiment, it is rather surprising for the FTW experiment taking into account the facts that (1) the FTW experiment corrects much of the erroneous SST gradient over the western Arabian Sea and that (2) many studies have suggested a key-role of the SST

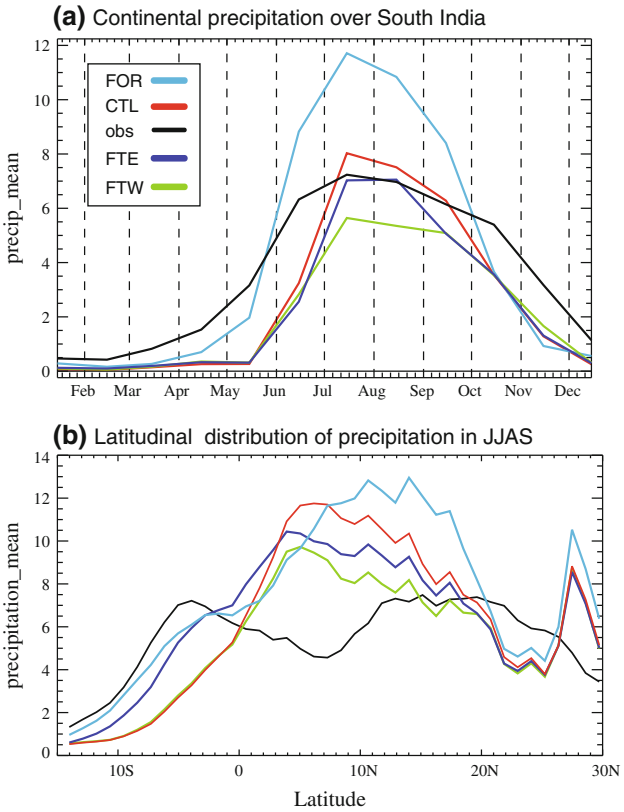

Fig. 8 **a** Monthly climatology of precipitation (in mm/day) over South India, averaged between 70–90°E/5–20°N over the land. **b** Latitudinal distribution of precipitation between 60 and 110°E (mm/day) during boreal summer (June to September). For all figures, observations are shown in black (precipitations are derived from TRMM from 1998 to 2010). CTL and FOR experiments are shown in *red* and *light blue*, respectively. FTW and FTE sensitivity experiments are in *green* and *dark blue*, respectively

warm pool or SST gradient over the Arabian Sea in controlling the ISM onset (e.g. Joseph et al. 2003; Sijikumar and Rajeev 2012). Since the SST corrections in FTW affect only the western Arabian Sea where SST biases are the strongest (particularly, during the onset period), one may wonder if the smaller SST errors in the eastern Arabian Sea, which are not corrected in FTW, may play a significant role in the delayed ISM onset (Masson et al. 2005, Levine and Turner 2012). In order to test this hypothesis, an additional sensitivity experiment has been carried out for 20 years, where the SST biases in the whole Arabian Sea (10–30°N 40–80°E) have been corrected. In this new experiment, the ISM evolution is not significantly different from the FTW and CTL experiments and the ISM onset is still delayed by more than 10 days (not shown). In other words, our numerical results suggest that the Arabian Sea SSTs play only a weak role in the delayed ISM onset in the CGCM. This unexpected result could be partly explained by the hypothesis formulated by Izumo et al. (2008 in their appendix C), where they suggest that the early part of the

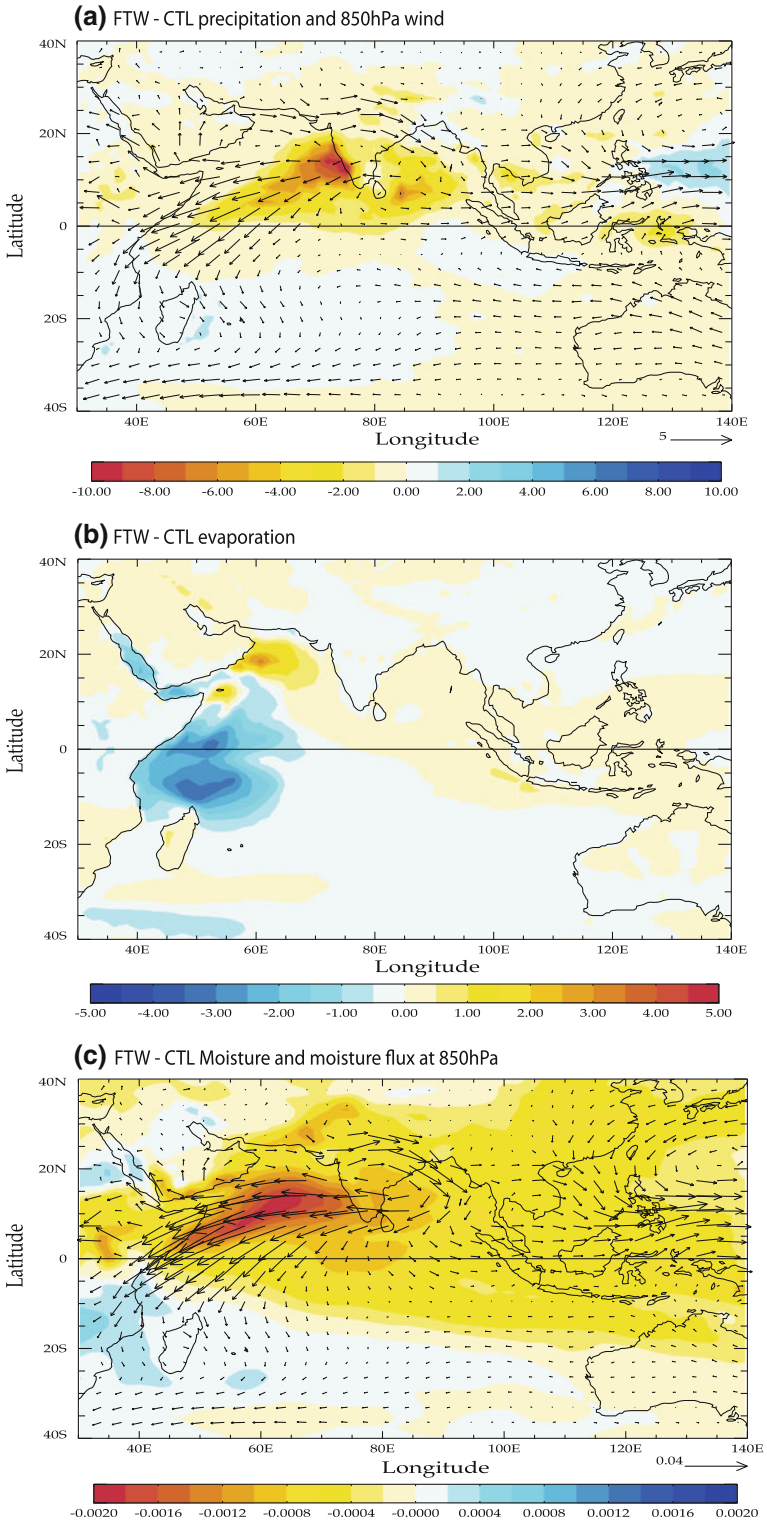

Fig. 9 Maps of differences between FTW and CTL experiments for ISM precipitation, 850 hPa wind and moisture. FTW minus CTL for climatological precipitations and 850 hPa winds from June to August. Precipitations are *shaded* (unit in mm/day with a contour interval of 1 mm/day). *Arrows* represent 850 hPa winds (scale in m/s at the *bottom right* of the plot). **a** FTW minus CTL for climatological evaporation (unit in mm/day, contour interval: 0.5 mm/day) from June to August. **b** FTW minus CTL for climatological moisture (e.g. specific humidity) and moisture flux at 850 hPa from June to August. Moisture at 850 hPa is *shaded* (in kg/kg with a contour interval of 0.002 kg/kg). *Arrows* represent moisture flux at 850 hPa (scale in kg/s/m^2 at the *bottom right* of the plot)

ISM is mostly controlled by variations in the wind field (and therefore the larger scale circulation) and not the SST in the Arabian Sea. Soman and Slingo (1997), using an atmosphere-only GCM, have obtained similar conclusions. Another possible hypothesis is that the SST gradient in the southwest Indian Ocean may also exert a strong control on the position of the ITCZ during boreal spring (Bollasina and Ming 2012).

4.1.2 ISM rainfall pattern and mean position of the ITCZ

We now focus on the ISM rainfall distribution and circulation errors during boreal summer in CTL and their possible relationships with the warm (cold) SST bias in the WIO (EIO). Figure 8b illustrates again the inability of the model, both in FOR and CTL, to reproduce the two observed locations of convection in the Indian region during boreal summer—the first one over the Indian subcontinent and the Bay of Bengal, the second over the eastern equatorial Indian Ocean (black curve in Fig 8b). Instead of these two precipitation maxima, all experiments simulate only one unique rainfall maximum, around 10°N in FOR and over 5°N in CTL and both sensitivity experiments.

Joseph et al. (2012) have suggested that the warm bias in the WIO is responsible of the biased TT gradient, which, in turn, is responsible of the wrong ITCZ position in the CTL simulation. In order to test this hypothesis, the TTG index, defined in Sect. 4.2.1 has been cumulated during the whole monsoon season, in order to measure the strength of ISM. The ISM strength remains constant in CTL (218 K) and FTW (219 K), which is still far from the observed value of 260 K. These results demonstrate that the WIO SST has also only a weak impact on the biased representation of the meridional TT gradient in the CGCM. Note that this result does not contradict the hypothesis that the overly weak meridional TT gradient in CTL is responsible of the wrong position of the ITCZ (Joseph et al. 2012).

However, Fig. 8a, b show that there is a significant impact of the correction of SST biases in both WIO and EIO regions on precipitation amplitude over Peninsular India and neighboring oceanic regions without changing the time evolution (e.g. Fig. 8a) or the shape of the meridional rainfall distribution (e.g. Fig. 8b) in the CGCM. In both sensitivity experiments, there is a significant decrease of precipitation in the northern hemisphere that is stronger in FTW than in FTE. In FTE, we observe also a reduction of the dry bias in the coupled run off Sumatra, around 5°S (see below).

4.1.3 Mechanisms in FTW

The decrease of SST in FTW causes an important reduction of monsoon moisture flux and precipitation, reaching −10 mm/day over western Arabian Sea and the Ghats (Fig. 9a). This decrease corrects the important excess of precipitation over the ocean, especially over the eastern Arabian Sea, we noticed in CTL, but at the expense of decreasing the low-level wind shear (Fig. 9a). As the dynamical strength of monsoon was correct in CTL (e.g. Figs. 4a, 5e), this reduction of the monsoon moisture flux in FTW enhances the lack of precipitation over India (Figs. 9a, 8a). Overall, these results are consistent with the studies of Levine and Turner (2012) and Izumo et al. (2008), which show that an increase (decrease) of SST in the WIO is associated with an increase (decrease) of monsoon rainfall in the HadGEM3 coupled model and the previous version of SINTEX-F model. This highlights the fact that the WIO is an important source of moisture for the ISM, at least in these models. Indeed, the mechanism we suggest to explain the decrease of rainfall over the eastern Arabian Sea and India in the FTW experiment is similar to the one put forward in these two studies: the decrease of SST in the WIO leads to an important decrease of evaporation over the WIO (Fig. 9b) and of specific humidity at 850 hPa over the whole North Indian Ocean (Fig. 9c). The maximum decrease of humidity occurs over the Arabian Sea and to a lesser extent over south of India and Bay of Bengal. This leads to a dramatic decrease of the moisture flux at low levels (Fig. 9c), which has an anticyclonic curvature over the Indian subcontinent, explaining the slowdown of the monsoon circulation in FTW.

4.1.4 Mechanisms in FTE

We observe a strong local response to the correction of the (cold) SST EIO biases, with a significant increase of precipitation over the EIO, which partly offsets the lack of precipitation observed over this region in CTL (Fig. 10a). However, this improvement leads to the same meridional rainfall distribution between 10°S and the equator (Fig. 8b) than in FOR. This suggests, once again, that the potential improvements linked to the SST corrections are limited by the atmospheric biases or that we need both the correct SST and the ocean–atmosphere feedbacks over the EIO in order to improve the simulated latitudinal rainfall distribution in the Indian sector.

Interestingly, Fig. 10a illustrates also a non-local response to the SST changes in the EIO with a significant decrease of precipitation north of the equator over the oceanic regions surrounding the Indian subcontinent (nearly one-third of the excess of ISM precipitation) and, to a much lesser extent, over India compared to CTL. Furthermore, these rainfall pattern modifications are associated with significant improvements of the inter-hemispheric monsoon flux in the central and eastern equatorial Indian Ocean, which are one of the major biases of the ISM circulation in CTL (see Fig. 10a and the previous section). Finally, these improvements extend and amplify during boreal fall with a partial correction of the rainfall and low-level wind components of the dipole-like pattern, seen in CTL (Fig. 10b).

The increased precipitation over the EIO in FTE is associated with more ascent over this region compensated by subsidence over the ocean regions surrounding

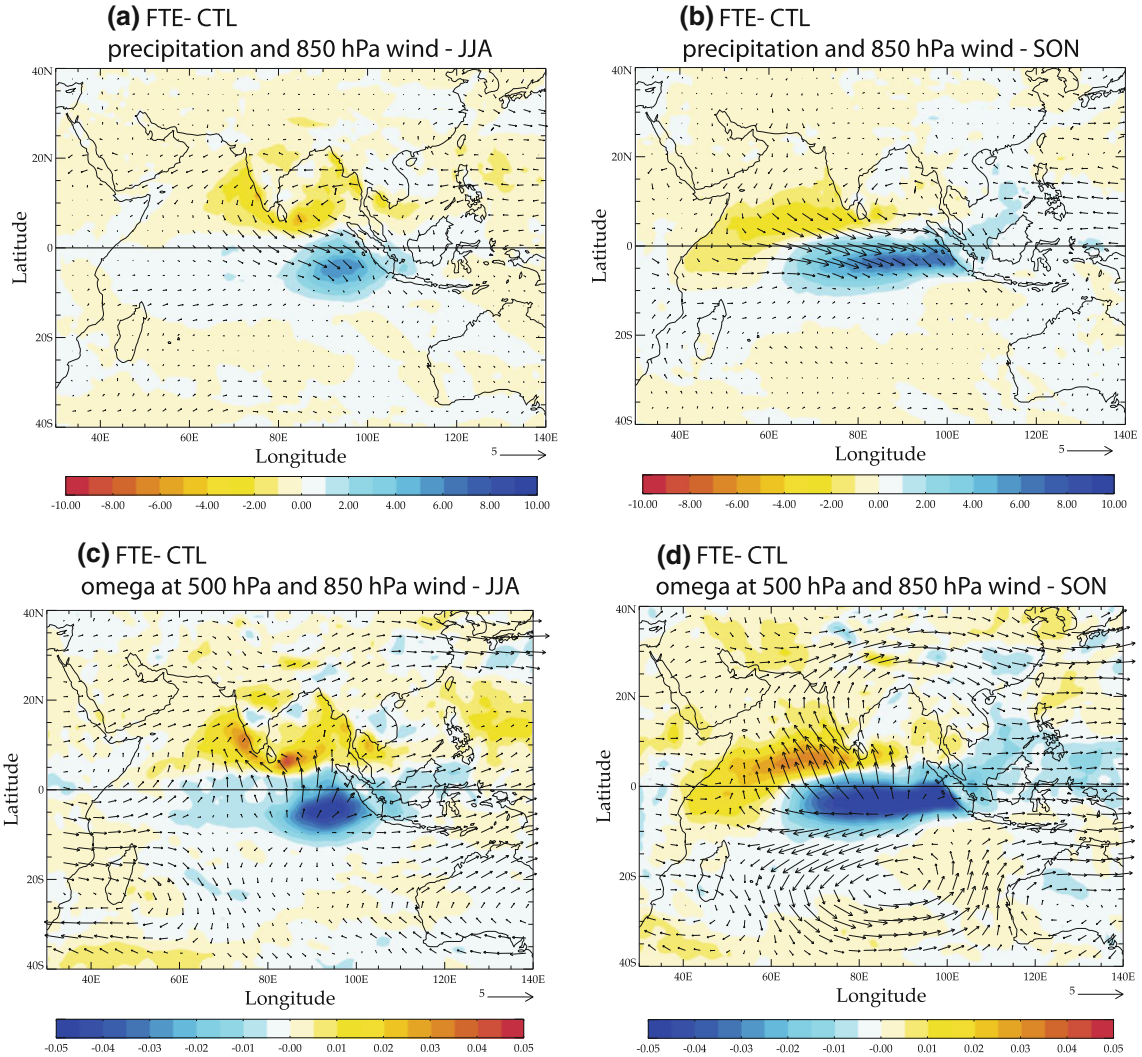

Fig. 10 Maps of differences between FTE and CTL experiments for ISM precipitation, low (850 hPa) and high (200 hPa) levels winds and vertical velocity (omega) at 500 hPa. **a** FTE minus CTL for climatological precipitations and 850 hPa winds during boreal summer (June to August). Precipitations are *shaded* (unit in mm/day with a contour interval of 1 mm/day). *Arrows* represent 850 hPa winds (scale in m/s at the *bottom right* of the plot). **b** Same as **a**, but for boreal fall (September to November). **c** FTE minus CTL for climatological omega at 500 and 200 hPa winds during boreal summer (June to August). Omega at 500 hPa is shaded (unit in Pa/s with a contour interval of 0.005 Pa/s). *Arrows* represent 200 hPa winds (scale in m/s at the *bottom right* of the plot). **d** Same as **c**, but for boreal fall (September to November)

peninsular India and an increased northward flux at 200 hPa (Fig. 10c, d). The non-local rainfall response in FTE is thus associated with a reorganization of the monsoon Hadley cell, induced solely by the changes of the EIO SSTs applied in FTE. This result, consistent with the works of Annamalai (2010) and Krishnan et al. (2000), highlights that the monsoon is partly thermally driven. However, it is important to keep in mind the key role played by the atmospheric biases (or alternatively the absence of coupling over the EIO in FTE) as the reduction of the EIO SSTs errors is (once again) not sufficient to restore the observed bimodal latitudinal structure of the monsoon rainfall (Fig. 8b).

To summarize our results about question (1), the corrections of the WIO and EIO SST biases do not impact the large-scale circulation errors in CTL, like the erroneous ITCZ location over the ocean near 5°N, nor the delayed ISM onset. The WIO area seems to be an important source of moisture for the ISM. The SST decrease in this region corrects an important part of the excess of precipitation over the ocean, but gives birth to new biases such as a lack of precipitation over south India and a too weak monsoon flux. On the other hand, the correction of the much smaller, but seasonally evolving cold SST bias in the EIO consistently restores a reasonable amount of precipitation in the EIO region, reduces significantly the excess of

precipitation over the ocean in the northern hemisphere and improves the equatorial low-level wind mean state. All these changes are interrelated through a modulation of the Hadley cell during boreal summer and fall, but the amplitude of the improvements seems to be limited by the atmospheric biases, the absence of coupling over the EIO (in the FTE experiment) or SST errors in other key oceanic regions for the monsoon (for a comprehensive review, see Wang 2006 or Gimeno et al. 2010).

4.2 Formation of dipole-like SST structure and associated circulation errors

The similarity between the seasonal evolution of the WIO and EIO SST biases in CTL (Fig. 7) and the formation of a positive IOD event (Chang et al. 2006; Drbohlav et al. 2007, their Fig. 4), suggests a comparable formation mechanism.

Figures 11a and b show the seasonal cycle of SST averaged in the WIO and EIO for the CTL and sensitivity experiments. Surprisingly, in both sensitivity experiments, the correction of the "local" SST errors does not have any significant impact on the seasonal evolution of the SST in the other region, especially during boreal summer and fall. Furthermore, the reduction of the warm WIO SST error in FTW is associated with colder EIO SST during all months, a feature that is not consistent with the tightly coupled evolution of the WIO and EIO SSTs during a positive dipole event. One of the key-elements in governing the evolution of positive dipole events is the equatorial Indian Ocean wind stress displayed in Fig. 11c (Fischer et al. 2005; Chang et al. 2006). In FTW, the correction of the WIO SST bias does not improve much the equatorial wind stress during summer and the correction is weak at best during autumn. These results are consistent with the weak atmospheric response simulated over the equatorial Indian Ocean during boreal summer in FTW (Fig. 9). During autumn, the correction of the equatorial zonal wind is also too weak to impact the thermocline depth (as inferred from d20, not shown). The absence of change in the oceanic mean state along the equator is consistent with the absence of change of SST on the opposite side of the basin.

In a similar fashion, there is no improvement of the WIO SST warm bias during both summer and autumn in FTE (Fig. 11a). But, Figs. 10b and 11c do show a significant atmospheric response to the EIO SST bias with a more realistic equatorial wind stress in FTE than in CTL. This in turn leads to an oceanic adjustment response, with a typical zonal dipole pattern in thermocline depth (deepening in the east, shallowing in the west), which slightly corrects the biased thermocline in CTL (see Fig. 5i). However, FTE equatorial wind stress is still affected by an easterly bias and remains westward instead of the strong eastward maximum observed during boreal fall (Fig 11c). Despite a slight improvement, the thermocline remains too deep in the west (not shown). This could explain why there is no significant improvement of the WIO warm bias in FTE (Fig. 11a). Interestingly, Fig. 11c illustrates that FOR is also affected by a similar westward equatorial wind stress bias during boreal fall. This suggests that, even during boreal fall, the atmospheric biases may control the evolution of the equatorial wind stress, and the associated biased thermocline in CTL. Further sensitivity experiments with more moderate flux adjustments (e.g. allowing some SST interannual and intraseasonal variability in the constrained region) are required to further confirm this hypothesis.

To conclude this section, the corrections of the SST WIO and EIO biases in the sensitivity experiments lead to improvements of the atmospheric circulation and rainfall distribution during boreal summer and fall, but without changing sufficiently the large-scale pattern of the biased atmospheric circulation or erroneous rainfall pattern in CTL. In other words, these SST biases seem only to induce a reinforcement of circulation biases already existing in FOR in most of the cases. Furthermore, all the improvements due to the SST corrections seem drastically limited by the atmosphere intrinsic biases, including prominently the unimodal oceanic position of the ITCZ and the enhanced westward wind stress along the equator. The correction of the SST in the WIO/EIO does not significantly impact the opposite side of the basin. This result contradicts the theory, suggested previously, that the formation of SST biases is due to a coupled mechanism, similar to the one occurring during the growth of a positive IOD event. On the other hand, the inability of the atmospheric model forced by the observed SSTs to reproduce an eastward wind stress along the equator during fall could explain the formation of these biases. Another hypothesis is that these biases are due to local coupled processes.

5 Conclusion and discussion

In this work, we therefore examine the impacts of SST biases on the ISM rainfall and the Indian Ocean mean state, in the SINTEX-F2 model, with the help of a comparison of forced and coupled control simulations and two sensitivity coupled experiments.

During boreal spring and winter, the coupled and forced simulations share many deficiencies. These common features suggest that, during boreal winter and spring, the main source of errors is coming from the atmospheric model, especially a dry islands bias in the Maritime Continent. The key-role of the Maritime Continent on atmospheric model biases was already highlighted by Neale and Slingo (2003). Conversely, during boreal summer and autumn, FOR and CTL exhibit significant mean state differences, suggesting a

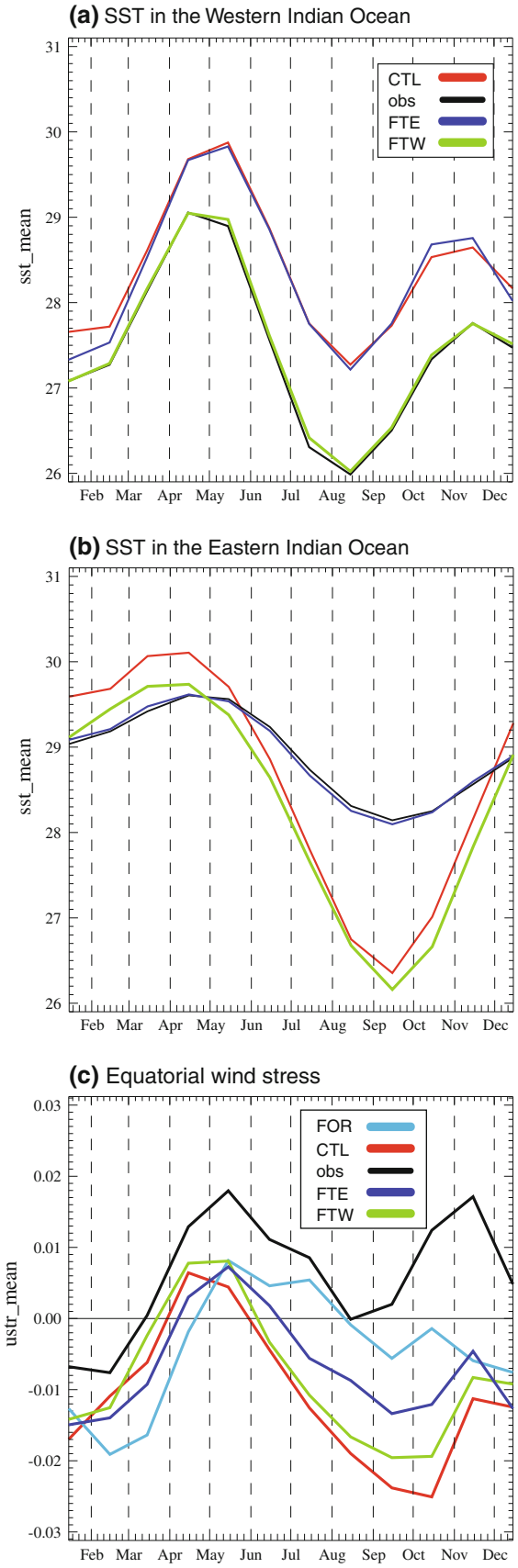

◀ **Fig. 11** Annual cycle of WIO and EIO SSTs and Indian Ocean equatorial wind stress in observations, FOR, CTL, FTW and FTE experiments. **a** Monthly climatology of SST (unit in °C) averaged in the WIO (35–60°E/10°S 30°N). **b** Monthly climatology of SST (unit in °C) averaged in the EIO (see Fig. 8 for definition). **c** Monthly zonal wind stress (N/m^2) averaged between 40°E–100°E and 5°S–5°N. For all figures, observations are shown in black (SST is derived from AVHRR from 1998 to 2010 and winds stress is derived from ERA interim from 1989 to 2009). CTL and FOR are shown in *red* and *light blue*, respectively. FTW and FTE sensitivity experiments are in *green* and *dark blue*, respectively

significant impact of the SST errors on the mean state of the coupled model. Therefore, in order to highlight the role of the Indian Ocean SST biases on the rainfall and atmospheric circulation, as well as the mutual interactions between these SST biases, two coupled sensitivity experiments have been designed, in which the SST biases are corrected either in the warm western (FTW) or cold eastern (FTE) Indian Ocean. Surprisingly and in spite of the correction of the SST biases, the large-scale pattern of the biased atmospheric circulation and rainfall distribution found in CTL is still evident in the two sensitivity experiments. Moreover, the emergence of these SST biases seem only to induce a reinforcement of circulation biases already existing in the atmosphere-only run, which include prominently a too southward and unimodal position of the ITCZ during boreal summer and a delayed southward migration of this ITCZ during boreal fall. This delayed transition of the ITCZ seems to play a key-role in the enhanced westward wind stress simulated along the equatorial Indian Ocean in all the experiments. These common features suggest again that deficiencies in the atmospheric model (e.g. convection) or missing land-vegetation processes may be responsible for these errors. Alessandri et al. (2007) showed a strong improvement in the monsoon representation, especially over India, when replacing, in the previous version of ECHAM (e.g. ECHAM4), the simple surface scheme by a land surface model. It remains, however, to be seen if such modifications will correct the above coupled model deficiencies.

Nevertheless, FTW experiment shows that the WIO is an important source of moisture for the ISM. The decrease (increase) of WIO SSTs leads to a global decrease (increase) of the ISM rainfall and strength consistent with the conclusions of Levine and Turner (2012), Izumo et al. (2008) and Gimeno et al. (2010). This modification is strongest over the southeastern Arabian Sea where it corrects a large part (and sometime even more) of the excess of oceanic precipitation in the CGCM. Meanwhile, it also decreases precipitation over India and monsoon strength, which was already slightly underestimated in the CGCM. Thus, the WIO SSTs seem to impact ISM via a "local" or regional evaporation effect rather than the modulation of the meridional temperature in the Indian region (Chung and Ramanathan 2006).

On the other hand, the correction of the cold SST bias in the EIO leads to a global improvement of the precipitation mean state via modulations of both the local Hadley and Walker circulations during boreal summer and fall. Despite the relatively small size of this area, it plays an important role on the Indian Ocean circulation, consistent with the work of Annamalai (2010). This cold EIO bias is common in many CGCMs (Lin 2007) and similar experiments with other coupled models could be interesting to confirm this result.

During boreal fall, both sensitivity experiments show that the correction of one SST bias does not have any significant impact on the other. This apparent de-connection could be explained by the inability of the atmospheric model to reproduce realistic equatorial winds along the equator during all the year. However, these results also suggest that the formation of these SST biases is mainly due to an oceanic local response to the atmospheric biases or to local coupled processes and not to an IOD-like mechanism in the framework of the SINTEX-F2 coupled model (Li et al. 2003; Spencer et al. 2005).

Nevertheless, several questions remain unanswered. First, the ISM onset date is significantly delayed in all coupled simulations, including the sensitivity experiments, whereas it is quite correct in the atmospheric run. This result is in contradiction with the study of Joseph et al. (2003) and Sijikumar and Rajeev (2012), but in accordance with Soman and Slingo (1997). In this last study, they suggested that the onset is mainly control by the West Pacific SSTs. Joseph et al. (1994), Boschat et al. (2011) and Levine and Turner (2012) have also suggested a remote impact of the Pacific SSTs on the onset. This problem will be investigated in a future work.

Second, the interannual variability has not been examined here. In both sensitivity experiments, the interannual variability has been suppressed in the corrected area. This could lead to important changes in the Indian and Pacific Ocean interannual variability. As an illustration, the sensitivity experiments could provide us some answers about the formation of the IOD and how Indian Ocean variability could impact ENSO variability (Luo et al. 2010, Izumo et al. 2010).

Acknowledgments A part of this research was supported by the Japan Science and Technology Agency/Japan International Cooperation Agency through the Science and Technology Research Partnership for Sustainable Development (SATREPS). This work was performed using HPC resources from GENCI-IDRIS (Grant 2012-x2012016895).

References

Dee DP et al (2011) The ERA-interim reanalysis: configuration and performance of the data assimilation system. Q J R Meteorol Soc 137:656, 553–597, Part A

Alessandri A, Gualdi S, Polcher J, Navarra A (2007) Effects of land surface–vegetation on the boreal summer surface climate of a GCM. J Clim 20:255–278. doi:10.1175/JCLI3983.1

Annamalai H (2010) Moist dynamical linkage between the Equatorial Indian Ocean and the South Asian monsoon trough. J Atmos Sci 67(3):589–610

Annamalai H, Murtugudde R (2004) Role of the Indian Ocean in regional climate variability. In: Wang C, Xie S-P, Carton JA (eds) Earth climate: the ocean-atmosphere interaction, vol 147. AGU Geophysical Monograph, Washington, DC, pp 213–246

Annamalai H, Liu P, Xie S-P (2005) Southwest Indian Ocean SST variability: its local effect and remote influence on Asian monsoons. J Clim 18:4150–4167

Annamalai H, Hamilton K, Sperber KR (2007) The South Asian summer monsoon and its relationship with ENSO in the IPCC AR4 simulations. J Clim 20:1071–1092. doi:10.1175/JCLI4035.1

Bollasina MA, Ming Y (2012) The general circulation model precipitation bias over the southwestern equatorial Indian Ocean and its implications for simulating the South Asian monsoon. Clim Dyn Online. doi:10.1007/s00382-012-1347-7

Bollasina MA, Nigam S (2009) Indian Ocean SST, evaporation, and precipitation during the South Asian summer monsoon in IPCCAR4 coupled simulations. Clim Dyn 33:1017–1032. doi:10.1007/s00382-008-0477-4

Boschat G, Terray P, Masson S (2011) Interannual relationships between Indian summer monsoon and Indo-Pacific coupled modes of variability during recent decades. Clim Dyn 37:1019–1043. doi:10.1007/s00382-010-0887-y

Boschat G, Terray P, Masson S (2012) Robustness of SST teleconnections and precursory patterns associated with the Indian summer monsoon. Clim Dyn 38:2143–2165. doi:10.1007/s00382-011-1100-7

Carton JA, Giese BS (2008) A reanalysis of ocean climate using simple ocean data assimilation (SODA). Mon Weather Rev 136:2999–3017

Chang C-P et al (2006) Climate fluctuations of tropical coupled systems—the role of ocean dynamics. J Clim 19:5122–5174

Cherchi A, Navarra A (2007) Sensitivity of the Asian summer monsoon to the horizontal resolution: differences between AMIP-type and coupled model experiments. Clim Dyn 28:273–290. doi:10.1007/s00382-006-0183-z

Chung CE, Ramanathan V (2006) Weakening of North Indian SST gradients and the monsoon rainfall in India and the Sahel. J Clim 19:2036–2045. doi:10.1175/JCLI3820.1

Compo GP, Whitaker JS, Sardeshmukh PD (2006) Feasibility of a 100-year reanalysis using only surface pressure data. Bull Am Meteorol Soc 87:175–190. doi:10.1175/BAMS-87-2-175

Drbohlav H-KL, Gualdi S, Navarra A (2007) A diagnostic study of the Indian Ocean Dipole mode in El Niño and Non–El Niño years. J Clim 20:2961–2977. doi:10.1175/JCLI4153.1

Fischer A, Terray P, Guilyardi E, Delecluse P (2005) Two independent triggers for the Indian Ocean Dipole/zonal mode in a coupled GCM. J Clim 18:3428–3449

Gill AE (1980) Some simple solutions for heat-induced tropical circulation. Q J R Meteorol Soc 106(449):447–462. doi:10.1002/qj.49710644905

Gimeno L, Drumond A, Nieto R, Trigo RM, Stohl A (2010) On the origin of continental precipitation. Geophys Res Lett 37(13):1–7. doi:10.1029/2010GL043712

Gualdi S, Guilyardi E, Navarra A, Masina S, Delecluse P (2003a) The interannual variability in the tropical Indian Ocean as simulated by a CGCM. Clim Dyn 20:567–582

Gualdi S, Navarra A, Guilyardi E, Delecluse P (2003b) Assessment of the tropical Indo-Pacific climate in the SINTEX CGCM. Ann Geophys 46:1–26

Guilyardi E, Delecluse P, Gualdi S, Navarra A (2003) Mechanisms for ENSO phase change in a coupled GCM. J Clim 16:1141–1158

Huffman GJ et al (1997) The global precipitation climatology project (GPCP) combined precipitation dataset. Bull Am Meteorol Soc 78:5–20

Izumo T, Montégut CB, Luo J–J, Behera SK, Masson S, Yamagata T (2008) The role of the western Arabian Sea upwelling in Indian monsoon rainfall variability. J Clim 21:5603–5623. doi: 10.1175/2008JCLI2158.1

Izumo T, Vialard J, Lengaigne M, De Boyer Montegut C, Behera SK, Luo J–J, Cravatte S, Masson S, Yamagata T (2010) Influence of the state of the Indian Ocean Dipole on the following year's El Niño. Nat Geosci 3(3):168–172

Joseph P, Eischeid JK, Pyle RJ (1994) Interannual variability of the onset of the Indian summer monsoon and its association with atmospheric features, El Niño, and sea surface temperature anomalies. J Clim 7:81–105

Joseph PV, Sooraj KP, Rajan CK (2003) Conditions leading to monsoon onset over Kerala and the associated Hadley cell. Mausam 54(1):155–164

Joseph S, Sahai AK, Goswami BN, Terray P, Masson S, Luo J–J (2012) Possible role of warm SST bias in the simulation of boreal summer monsoon in SINTEX-F2 coupled model. Clim Dyn 38:1561–1576. doi:10.1007/s00382-011-1264-1

Koch-Larrouy A, Madec G, Bouruet-Aubertot P, Gerkema T, Bessières L, Molcard R (2007) On the transformation of Pacific Water into Indonesian throughflow water by internal tidal mixing. Geophys Res Lett 34:L04604. doi:10.1029/2006GL028405

Kripalani RH, Oh JH, Kulkarni A, Sabade SS, Chaudhari HS (2007) South Asian summer monsoon precipitation variability: coupled climate model simulations and projections under IPCC AR4. Theor Appl Climatol 90:133–159. doi:10.1007/s00704-006-0282-0

Krishnan R, Zhang C, Sugi M (2000) Dynamics of breaks in the Indian summer monsoon. J Atmos Sci 1969:1354–1372

Kumar KK, Hoerling M, Rajagopalan B (2005) Advancing dynamical predictions of the Indian monsoon rainfall. Geophys Res Lett 32:L08704. doi:10.1029/2004GL021979

Kummerow C et al (2001) The evolution of the goddard profiling algorithm (GPROF) for rainfall estimation from passive microwave sensors. J Appl Meteorol 40:1801–1820

Levine RC, Turner AG (2012) Dependence of Indian Monsoon rainfall on moisture fluxes across the Arabian Sea and the impact of coupled model sea surface temperature biases. Clim Dyn 38:2167–2190. doi:10.1007/s00382-011-1096-z

Li T, Wang B, Chang C-P, Zhang Y (2003) A theory for the Indian Ocean Dipole–zonal mode. J Atmos Sci 60:2119–2135

Lin J-L (2007) The double-ITCZ problem in IPCC AR4 coupled GCMs: ocean–atmosphere feedback analysis. J Clim 20:4497–4525

Loschnigg J, Meehl G, Webster P, Arblaster J, Compo G (2003) The Asian Monsoon, the tropical biennial oscillation, and the Indian Ocean zonal mode in the NCAR CSM. J Clim 16:1617–1642

Luo J–J, Masson S, Behera SK, Delecluse P, Gualdi S, Navarra A, Yamagata T (2003) South Pacific origin of the decadal ENSO-like variation as simulated by a coupled GCM. Geophys Res Lett 30:2250. doi:10.1029/2003GL018649

Luo JJ, Masson S, Behera SK, Shingu S, Yamagata T (2005) Seasonal climate predictability in a coupled OAGCM using a different approach for ensemble forecasts. J Clim 18:4474–4497. doi: 10.1175/JCLI3526.1

Luo J–J, Zhang R, Behera SK, Masumoto Y, Jin FF, Lukas R, Yamagata T (2010) Interaction between El Niño and Extreme Indian Ocean dipole. J Clim 23:726–742

Madec G (2008) NEMO ocean engine. Note du Pôle de modélisation, Institut Pierre-Simon Laplace (IPSL), France. No 27. ISSN No 1288-1619

Madec G, Delecluse P, Imbard M, Levy C (1998) OPA 8.1 ocean general circulation model reference manual. Note du Pôle de modélisation, Institut Pierre-Simon Laplace (IPSL), France. No 11, 91 pp. Available at http://www.lodyc.jussieu.fr/NEMO/general/manual/Doc_OPA8.1.pdf

Masson S, Luo JJ, Madec G, Vialard J, Durand F, Gualdi S, Guilyardi E, Behera S, Delecluse P, et al (2005) Impact of barrier layer on winter-spring variability of the southeastern Arabian Sea. Geophys Res Lett 32: L07703, 1–4

Masson S, Terray P, Madec G, Luo J–J, Yamagata T, Takahashi K (2012) Impact of intra-daily SST variability on ENSO characteristics in a coupled model. Clim Dyn 39:681–707. doi: 10.1007/s00382-011-1247-2

Neale R, Slingo J (2003) The maritime continent and its role in the global climate: a GCM study. J Clim 16:834–848

Nordeng TE (1994) Extended versions of the convective parameterization scheme at ECMWF and their impact on the mean and transient activity of the model in the tropics. ECMWF Research Dept. Tech. Memo. 206, European Centre for Medium-Range Weather Forecasts, Reading, United Kingdom, 41 pp

Reynolds RW, Smith TM, Liu C, Chelton DB, Casey KS, Schlax MG (2007) Daily high-resolution blended analyses for sea surface temperature. J Clim 20:5473–5496

Roeckner E, Alfred S, Amala Y (1996) The atmospheric general circulation model ECHAM-4: model description and simulation of present-day climate. Max-Planck-Institut für Meteorologie. Report no. 218, 94 pp, Hamburg

Roeckner E, Baüml G, Bonaventura L, Brokopf R, Esch M, Giorgetta M, Hagemann S et al (2003) The atmospheric general circulation model ECHAM5: Part 1: model description. Max-Planck-Institut für Meteorologie, MPI-Report 353, Hamburg

Roeckner E, Brokopf R, Esch M, Giorgetta M, Hagemann S, Kornblueh L, Manzini E, Schlese U, Schulzweida U (2004) The atmospheric general circulation model ECHAM5 Part II: sensitivity of simulated climate to horizontal and vertical resolution. Max-Planck-Institute for Meteorology, MPI-Report 354, Hamburg

Schott FA, McCreary JP Jr (2001) The monsoon circulation of the Indian Ocean. Prog Oceanogr 51:1–123

Schott F, Fischer J, Garternicht U, Quadfasel D (1997) Summer monsoon response of the northern Somali Current, 1995. Geophys Res Lett 24:2565–2568

Shukla J, Hagedorn R, Hoskins B, Kinter J, Marotzke J, Miller M, Palmer TN, Slingo J (2009) Revolution in climate prediction is both necessary and possible: a declaration at the world modelling summit for climate prediction. Bull Am Meteorol Soc 90:175–178

Sijikumar S, Rajeev K (2012) Role of the Arabian Sea Warm Pool on the precipitation characteristics during the monsoon onset period. J Clim 25:1890–1899. doi:10.1175/JCLI-D-11-00286.1

Soman MK, Slingo JM (1997) Sensitivity of the Asian summer monsoon to aspects of sea-surface-temperature anomalies in the tropical Pacific. Q J R Meteorol Soc 123:309–336

Spencer H, Sutton RT, Slingo JM, Roberts JM, Black E (2005) The Indian Ocean climate and dipole variability in the Hadley centre coupled GCMs. J Clim 18:2286–2307

Terray P, Guilyardi E, Fischer AS, Delecluse P (2005) Dynamics of the Indian Monsoon and ENSO relationships in the SINTEX global coupled model. Clim Dyn 24:145–168

Terray P, Chauvin F, Douville H (2007) Impact of southeast Indian Ocean sea surface temperature anomalies on monsoon-ENSO-dipole variability in a coupled ocean-atmosphere model. Clim Dyn 28:553–580. doi:10.1007/s00382-006-0192-y

Terray P, Kamala K, Masson S, Madec G, Sahai AK, Luo J–J, Yamagata T (2012) The role of the intra-daily SST variability in the Indian Monsoon variability and monsoon-ENSO–IOD relationships in a global coupled model. Clim Dyn 39:729–754. doi: 10.1007/s00382-011-1240-9

Tiedtke M (1989) A comprehensive mass flux scheme for cumulus parameterization in large-scale models. Mon Weather Rev 117:1779–1800

Timmermann R, Goosse H, Madec G, Fichefet T, Ethe C, Duliere V (2005) On the representation of high latitude processes in the ORCA-LIM global coupled sea ice-ocean model. Ocean Model 8(1–2):175–201

Valcke S (2006) OASIS3 user guide (prism_2-5). PRISM support initiative report No 3, 64 pp

Wang B (2006) The Asian Monsoon. Springer/Praxis Publishing, New York, p 787

Wang B, Wu R, Lau KM (2001) Interannual variability of the Asian summer monsoon: contrast between the Indian and the Western North Pacific–East Asian monsoons. J Clim 14:4073–4090

Wang B, Kang I, Lee J (2004) Ensemble simulations of Asian–Australian monsoon variability by 11 AGCMs. J Clim 17:803–818

Wang B, Ding QH, Fu XH, Kang I-S, Jin K, Shukla J, Doblas-Reyes F (2005) Fundamental challenge in simulation and prediction of summer monsoon rainfall. Geophysl Res Lett 32:L15711

Wang B, Lee JY, Kang IS, Shukla J, Kug JS, Kumar A, Schemm J, Luo JJ, Yamagata T, Park CK (2008) How accurately do coupled climate models predict the leading modes of Asian-Australian monsoon interannual variability? Clim Dyn 30:605–619. doi: 10.1007/s00382-007-0310-5

Wentz FJ, Gentemann C, Smith D, Chelton D (2000) Satellite measurements of sea surface temperature through clouds. Science 288:847

Wu RG, Kirtman BP (2005) Roles of Indian and Pacific Ocean air-sea coupling in tropical atmospheric variability. Clim Dyn 25:155–170

Xavier PK, Marzin C, Goswami BN (2007) An objective definition of the Indian summer monsoon season and a new perspective on the ENSO-Monsoon relationship. Q J R Meteorol Soc 133:749–764

Yokoi T, Tozuka T, Yamagata T (2008) Seasonal variation of the Seychelles Dome. J Clim 21:3740–3754. doi:10.1175/2008JCLI1957.1